Stratospheric ozone intrusion events and their impacts on tropospheric ozone

Jesse Greenslade[1], Simon Alexander[2], Robyn Schofield[3,4], Jenny A. Fisher[1,5], and Andrew Klekociuk[2]

[1]Centre for Atmospheric Chemistry, School of Chemistry, University of Wollongong
[2]Australian Antarctic Division, Hobart
[3]School of Earth Sciences, University of Melbourne
[4]ARC Centre of Excellence for Climate System Science, University of New South Wales
[5]School of Earth & Environmental Sciences, University of Wollongong

Correspondence to: Jesse Greenslade (jwg366@uowmail.edu.au)

Abstract. We develop a quantitative method to identify Stratosphere to Troposphere Transport events (STTs) from ozonesonde profiles. Using this method we estimate the seasonality and quantity of ozone transported across the tropopause over Melbourne (38°S), Macquarie Island (54°S), and Davis (69°S). STT seasonality is determined by two distinct methods using 7–9 years of ozone profiles from each site. The primary method we focus on here shows STT events frequently occurring during summer above all three sites. The majority of tropospheric ozone peaks from by STT events occur within 3 km below the tropopause at Melbourne and Macquarie Island, and within 2 km below the tropopause at Davis. Overall, the fraction of total tropospheric ozone attributed to STT events is 2 – 4% at each site, however, during individual events, an STT event can contribute more than 10% of the total tropospheric ozone at that time. The meteorological cause of STT events is postulated through visual inspection of ERA-I weather data, with the majority of events caused by low pressure frontal systems at all three sites. Ozone enhancements caused by transported biomass burning plumes are flagged after analysis of CO column measurements from the AIRS satellite. We use the GEOS-Chem model to understand our point-source ozonesonde results in a 3-dimensional context. The GEOS-Chem model is run with active stratospheric chemistry, and is too coarsely resolved in the vertical dimension to determine STTs. Simulated seasonal cycles of tropospheric ozone are well matched at all three sites although vertical profile averages have some bias in the troposphere compared with ozonesondes. A conservative estimate of yearly tropospheric ozone flux due to STTs are calculated using the simulated tropospheric ozone column between 35°S and 75°S of 3.2×10^{16} molecules cm^{-2} yr^{-1}. Using an assumed STT impact (of 30%) over the southern ocean rather than our conservative calculation increases the flux estimate to ∼30.2 Tg yr^{-1}.

1 Introduction

Tropospheric ozone constitutes only 10% of the total ozone column but is an important oxidant and greenhouse gas which is toxic to life, harming natural ecosystems and reducing agricultural productivity. Over the industrial period, increasing tropospheric ozone has been estimated to exert a radiative forcing equivalent to a quarter of the CO_2 forcing (Forster et al., 2007). Further tropospheric ozone enhancements are projected to drive reductions in global crop yields equivalent to losses of up to

USD_{2000}$ 35 billion per year by 2030 (Nawahda, 2013), along with detrimental health outcomes equivalent to $\sim$$USD$_{2000}$11.8 billion per year by 2050 (Selin et al., 2009). Tropospheric ozone is produced photochemically from NO_x and volatile organic compounds, which have both anthropogenic (fossil fuel, biomass combustion) and natural (wildfires, lightning, biogenic) sources. In the upper troposphere, downward transport from the ozone-rich stratosphere provides an additional natural source of tropospheric ozone (Jacobson and Hansson (2000) and references therein).

Stratosphere-to-troposphere transport (STT) primarily impacts the ozone budget in the upper troposphere but can also increase regional surface ozone levels above the legal thresholds set by air quality standards (Danielsen, 1968; Lefohn et al., 2011; Langford et al., 2012; Zhang et al., 2014). In the western US, for example, STT events have been shown to contribute up to 30% of surface ozone in spring (Lin et al., 2012). Estimates of the overall contribution of STT to tropospheric ozone vary widely (e.g., (Galani, 2003), Stohl et al. (2003), Stevenson et al. (2006), Lefohn et al. (2011)). A review of two photochemical models by Stohl et al. (2003) concluded that 25-50% of the tropospheric ozone column can be attributed to STT events globally, with most contribution in the upper troposphere. In contrast, Stevenson et al. (2006) found STT was responsible for only $\sim$ 10% of the tropospheric ozone column (equivalent to 550 ± 170 Tg yr^{-1}) in the Atmospheric Chemistry and Climate Model Inter-comparison Project (ACCMIP) simulations, with the remainder produced photochemically. This wide range in model estimates exists in part because STT is challenging to accurately represent in models. Observation-based process studies are therefore key in determining the relative frequency of STT events, with models then able to use this to quantify STT impact over large regions. Ozonesondes are particularly valuable for this purpose as they provide multi-year datasets with high vertical resolution.

Lower stratospheric and tropospheric ozone concentrations are highly correlated (Terao et al., 2008), suggesting mixing across the tropopause mainly caused by the jet streams over the ocean. Extratropical STT events most commonly occur during synoptic-scale tropopause folds (Sprenger et al., 2003; Tang and Prather, 2012; Frey et al., 2015) and are characterised by tongues of high potential vorticity (PV) air descending to low altitudes. As these tongues become elongated, filaments disperse away from the tongue and mix irreversibly into the troposphere. The strength (ozone enhancement above background levels), horizontal scale, vertical depth, and longevity of these intruding ozone tongues vary with weather, topography, and season. STT events have been observed in tropopause folds around both the polar front jet (Vaughan et al., 1993; Beekmann et al., 1997) and the subtropical jet (Baray et al., 2000). They are also observed near cut-off lows (Price and Vaughan, 1993; Wirth, 1995), implying the associated turbulent weather may induce stratospheric mixing.

STT events are driven by deep overshooting convection (Frey et al., 2015), tropical cyclones (Das et al., 2016) and mid-latitude synoptic scale disturbances (e.g. Stohl et al. (2003); Mihalikova et al. (2012)) and are strongly dependent on both season and location. While the frequency, seasonality, and impacts of STT events have been well characterised in the tropics and Northern Hemisphere (NH), observational estimates from the Southern Hemisphere (SH) extra-tropics are noticeably absent from the literature. Since 1998 NASA has tried to standardise ozonesonde release procedures and improve measurement frequency in the SH through the Southern Hemisphere ADditional OZonesonde (SHADOZ) program (http://croc.gsfc.nasa.gov/shadoz/). The SHADOZ ozonesondes were recently used to show increasing upper tropospheric ozone near southern Africa, most likely due to stratospheric mixing (Liu et al., 2015; Thompson et al., 2014). Nonetheless, the role of STT in the

Table 1. Seasonal distribution of sonde releases per site.

Site	Sondes	Sondes by month (JFMAM...)	Start to end date
Davis	240	11,12,13,12,17,31,29,28,32,28,15,12	2006/04/13 - 2013/11/13
Macquarie	390	32,31,45,28,34,33,28,35,29,33,31,31	2004/01/20 - 2013/01/09
Melbourne	456	31,38,40,38,41,36,38,39,46,40,38,31	2004/01/08 - 2013/12/18

SH remains highly uncertain due to the much more limited ozonesonde release sites compared to the NH and temporal sparsity in these datasets (Liu et al., 2015; Thompson et al., 2014; Mze et al., 2010). While many of the ozonesonde releases only occur every two to four weeks, ozone intrusion events often last for just a matter of hours (Tang and Prather, 2012).

Here, we characterise the seasonal cycle of STT events and quantify their contribution to the tropospheric ozone budget using nearly a decade of ozonesonde observations from three locations around the Southern Ocean spanning latitudes from 38°S - 69°S. In Section 2 we describe the observations and the methods used to identify STT events and to relate STT occurrence to meteorological events. Section 3 provides our newly derived climatologies of STT frequency, seasonality, intrusion altitude, and depth, and Section 4 uses these new climatologies to evaluate upper tropospheric ozone in a global chemical transport model (GEOS-Chem). Finally, in Section 5 we use the observations and the model to estimate the overall contribution of STT events to total tropospheric ozone in the high southern latitudes.

2 Data and Methods

2.1 Ozonesonde record in the Southern Ocean

Ozonesondes provide a high vertical resolution profile of ozone, temperature, pressure, and humidity from the surface to 35 km.

Ozone mixing ratio is quantified with an electrochemical concentration cell that senses the proportional electrical current from reaction of ozone with a solution of potassium iodide. Standardised procedures are followed when constructing, transporting, and releasing the ozonesondes (NOAA). Ozonesondes are estimated to provide around 2% precision in the stratosphere, which improves at lower altitudes (NOAA), and ozonesondes have been shown to be accurate to within 5% when the correct procedures are followed (Smit et al., 2007).

Ozonesondes are launched approximately weekly from Melbourne (38°S, 145°E), Macquarie Island (55°S, 159°E) and Davis (69°S, 78°E). For this study, we use the data collected from 2004-2013 for Melbourne and Macquarie, and 2006-2013 for Davis because both ozone and geopotential height (GPH) profiles were measured during these periods. At Davis, ozonesondes are launched twice as frequently during the ozone hole season and preceding months (June-October) as at other times of year (Alexander et al., 2013). A summary of ozonesondes at each site can be seen in table 1.

Characterisation of STT events requires a clear definition of the tropopause. The two most common tropopause height definitions are the standard lapse rate tropopause (WMO, 1957) and the ozone tropopause (Bethan et al., 1996). The lapse

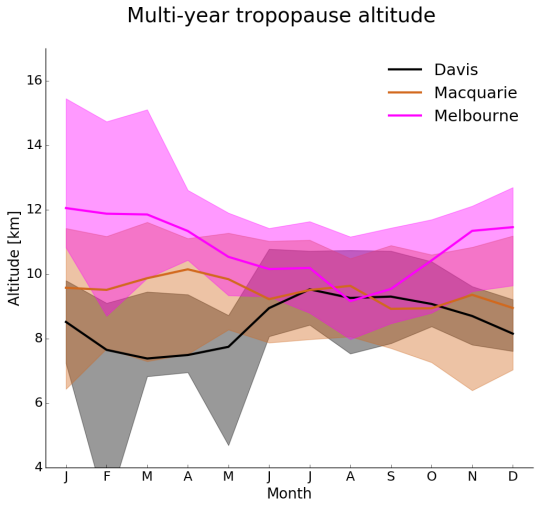

Figure 1. Multi-year monthly median tropopause altitude (minimum of lapse rate and ozone defined tropopause) determined from ozonesondes measurements at Melbourne (2004-2013), Macquarie (2004-2013) and Davis (2006-2013) (solid lines). Vertical shading shows the 10th to the 90th percentile of tropopause altitude for each site.

rate tropopause is defined as the lowest altitude where the lapse rate (vertical gradient of temperature) is less than 2°C km^{-1}, provided the lapse rate between this altitude and 2 km above is also below 2°C km^{-1}. The ozone tropopause is defined as the lowest altitude satisfying the following three conditions for the ozone mixing ratio (OMR) (Bethan et al., 1996):

1. Vertical gradient of OMR is greater than 60 ppb km^{-1};
2. OMR is greater than 80 ppb; and
3. OMR exceeds 110 ppb between 500 m and 2000 m above the altitude under inspection (500 m and 1500 m in the Antarctic, including the site at Davis).

The ozone tropopause can be less robust during stratosphere-troposphere exchange; however, it is more robust than the lapse rate tropopause at polar latitudes in winter and near jet streams in the lower stratosphere due to temperature inversions near the tropopause (Bethan et al., 1996; Tomikawa et al., 2009; Alexander et al., 2013). In this work, the lower of these two tropopause altitudes is used. This choice avoids occasional unrealistically high tropopause heights due to perturbed ozone or temperature measurements in the ozonesonde data.

Figure 1 shows the monthly mean tropopause altitudes at each location (solid lines). At Melbourne, tropopause altitude displays a seasonal cycle with maximum in summer and minimum is winter. This seasonality is missing at Macquarie and almost reversed at Davis, which has a minimum during autumn and maximum from winter to spring. Tropopause altitude decreases with latitude from 9-12 km at Melbourne (38°S) to 7-9 km at Davis (69°S).

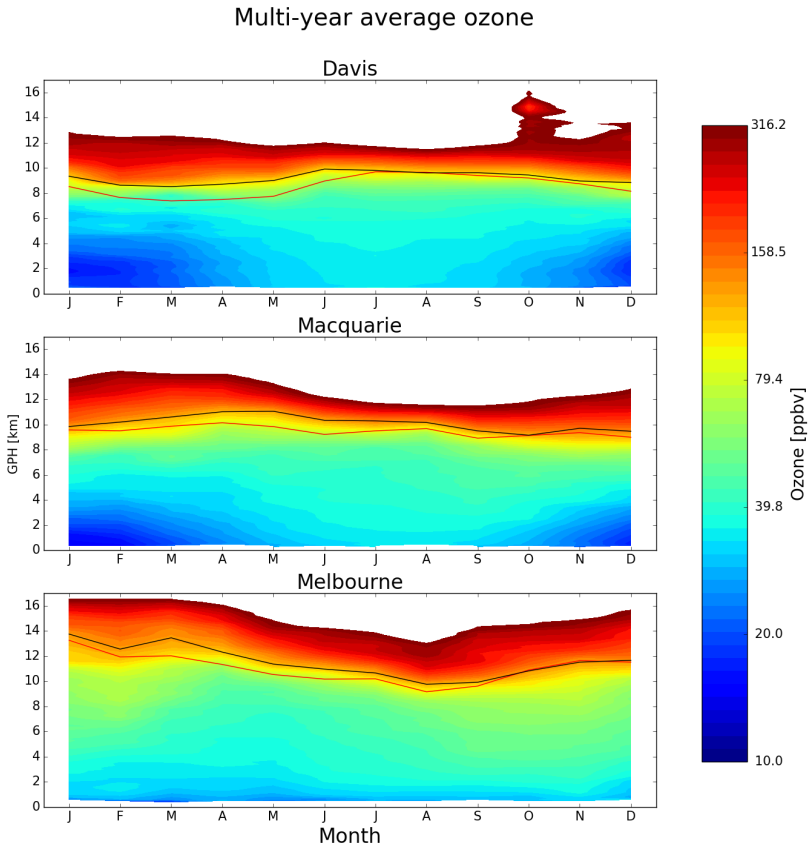

Figure 2. Multi-year mean seasonal cycle of ozone mixing ratio over Davis, Macquarie, and Melbourne as measured by ozonesondes. Measurements were interpolated to every 100 m and then binned monthly. Black and red solid lines show median ozone and lapse-rate defined tropopause altitudes (respectively), defined as described in the text.

Figure 2 shows multi-year averaged ozone mixing ratios measured by ozonesonde over the three stations. Over Melbourne, increased ozone extending down through the troposphere is apparent from December to March and from September to November. The increased tropospheric ozone in these months is due to STT (in summer), and possible biomass burning influence (in winter), both discussed in more detail below. Over Davis and Macquarie Island, tropospheric ozone is higher between March and October, although the seasonal differences are small compared to those at Melbourne. This seasonality at the high latitude sites is driven by a decrease in photochemical destruction under the reduced radiation conditions around polar night (TODO: read and cite S. Oltmans antarctic papers - re Andrews comment).

2.2 Model description

To provide regional context to the ozonesonde observations, we use the GEOS-Chem version 10-01 global chemical transport model (Bey et al., 2001), which simulates ozone along with more than 100 other trace gases throughout the troposphere and stratosphere. Stratosphere-troposphere coupling is calculated using the stratospheric unified chemistry extension (UCX) (Eastham et al., 2014). Transport is driven by assimilated meteorological fields from the Goddard Earth Observing System (GEOS-5) maintained by the Global Modeling and Assimilation Office (GMAO) at NASA. Ozone precursor emissions are from the Model of Emissions of Gases and Aerosols from Nature (MEGAN) version 2.1 (Guenther et al., 2012) for biogenic species and from the Emissions Database for Global Atmospheric Research (EDGAR) version 4.2 for anthropogenic species. Simulated biomass burning production is driven by the Global Fire Emissions Database (GFED4) inventory. Our simulation was modified from the standard v10-01 to fix a bug in the treatment of Total Ozone Mapping Spectrometer (TOMS) satellite data used to calculate photolysis (see http://wiki.seas.harvard.edu/geos-chem/index.php/FAST-JX_v7.0_photolysis_mechanism#Fix_for_TOMS_to_address_strange_cycle_in_OH_output.).

Our simulations span 2005-2012 (following a 1-year spin-up for 2004) with horizontal resolution of 2° latitude by 2.5° longitude and 72 vertical levels from the surface to 0.01 hPa. For comparison to the ozonesonde observations, the model was sampled every 6 hours within the grid box containing each site. When comparing against ozonesondes, GEOS-Chem UTC+0 time samples are used for all sites. This means that the simulated ozone profiles are analysed at local times of 7AM for Davis, and 11AM for Macquarie and Melbourne.

2.3 Characterisation of STT events and associated fluxes

We characterise STT events using the ozonesonde vertical profiles to identify tropospheric ozone enhancements above a local background (in moles per billion moles of dry air, referred to here as ppb). The process is illustrated in Figure 3 for an example ozone profile. First, the ozone vertical profiles are linearly interpolated to a regular grid with 20 m resolution from the surface to 14 km altitude. The interpolated profiles are then bandpass-filtered using a Fourier transform to retain perturbations with vertical scales between 0.5 km and 5 km (removing low and high frequency perturbations). In what follows, these filtered vertical profiles are referred to as perturbation profiles. The choice of band limits was set empirically. For an event to qualify as STT, a clear increase above the background ozone level is needed, and we find that a vertical limit of ~ 5 km removes seasonal-scale effects. The 0.5 km scale limit is set in order to remove any spikes of ozone which could be considered noise. We next use all the perturbation profiles at each site to calculate the 99th percentile perturbation value for the site. This is considered our threshold for tropospheric ozone perturbations, and perturbations above this threshold in individual ozonesondes are classified as STT events. STT events at altitudes below 4 km are removed to avoid surface pollution, and events within 0.5 km of the tropopause are removed to avoid spurious false positives induced by the sharp transition to stratospheric air.

We define the ozone peak as the altitude where the OMR is greatest within the lowest range of altitudes over which the perturbation profile exceeds the percentile-based threshold. The STT event is confirmed If the perturbation profile drops below zero between the ozone peak and the tropopause. Alternatively, the STT event is also confirmed if the OMR between the ozone

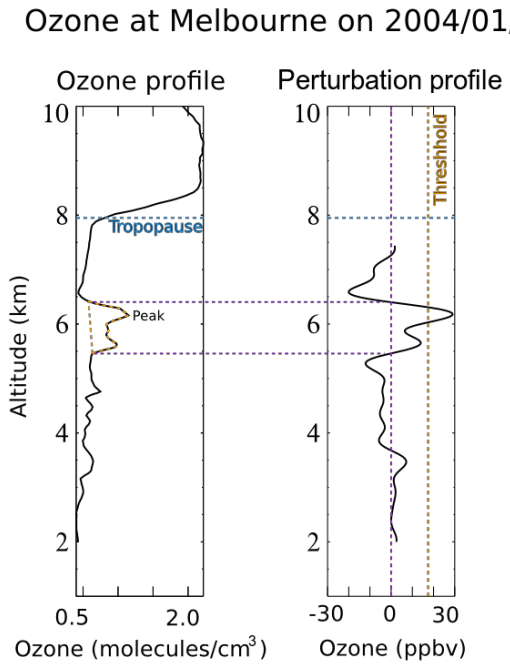

Figure 3. An example of the STT identification and flux estimation methods used in this work. The left panel shows an ozone mixing ratio profile from Melbourne on 8 January 2004 from 2km to the tropopause (dashed horizontal line). The right panel shows the perturbation profile created from bandpass filtering of the mixing ratio profile. The STT occurrence threshold calculated from the 99th percentile of all perturbation profiles is shown as the orange dashed line, and the vertical extent of the event is shown with the purple dashed lines (see details in text). The ozone flux associated with the STT event is calculated using the area outlined with the orange dashed line in the left panel.

peak and the tropopause drops below 80 ppb and is at least 20 ppb lower than the OMR at the ozone peak. If neither of these conditions are met, the profile is rejected as a non-event. This final step removes near-tropopause anomalies for which there is no evidence of detachment from the stratosphere. Vertical ozone profile recorded by ozonesondes are highly dependent on the time of launch (Sprenger et al., 2003), and it cannot be guaranteed that detected ozone enhancements are fully separated from the stratosphere, although this method minimises that risk by removing detected events too near the tropopause.

We estimate the ozone flux into the troposphere associated with each event by integrating the ozone concentration enhancement vertically over the altitude range for which an STT event is identified (i.e. enhancement near the ozone peak over which the perturbation profile is greater than zero). This estimate is conservative because it does not take into account any secondary ozone enhancements that may have been caused by the STT, and also ignores any enhanced ozone background amounts from synoptic-scale stratospheric mixing into the troposphere.

Our method differs somewhat from that used by Tang and Prather (2010) to detect STT events from ozonesonde measurements. Their definition is based on subjective analysis of sondes released from 20 stations ranging in latitude from 35°S to

40°N. They identify an STT event if, starting from 5 km altitude, ozone exceeds 80 ppb and then within 3 km decreases by 20 ppb or more to a value less than 120 ppb.

2.4 Biomass burning influence

The STT detection algorithm described in Section 2.3 assumes all mid-upper troposphere ozone perturbations above the 99th percentile are caused by stratospheric intrusions. In some cases, however, these perturbations may in fact reflect ozone production in lofted smoke plumes. Biomass burning in southern Africa and South America has previously been shown to have a major influence on atmospheric composition in the vicinity of our measurement sites (Oltmans et al., 2001; Gloudemans et al., 2007; Edwards et al., 2006), particularly from July to December (Pak et al., 2003; Liu et al., 2016). On occasion, smoke plumes from Australian and Indonesian fires can also reach the mid-high southern latitudes, as seen from satellite measurements of carbon monoxide (CO) discussed below.

Large biomass burning events emit substantial quantities of ozone precursors, some of which are capable of being transported long distances and driving ozone production far from the fire source (Jaffe and Wigder, 2012). Ozone production from biomass burning is complex and affected by photochemistry, fuel nitrogen load, and time since emission, among other factors. While ozone production occurs in some biomass burning plumes, this is not always the case; therefore ozone perturbations detected during transported smoke events may or may not be caused by the plume. We therefore flag all detected STT events found near smoke plumes but do not exclude them from our final dataset.

Possible biomass burning influence is identified using satellite observations of CO from the AIRS (Atmospheric Infrared Sounder) instrument on board the Aqua satellite (Texeira, 2013). CO is emitted during incomplete combustion and is an effective tracer of long-range transport due to its long lifetime. In the Southern Hemisphere, biomass burning is the primary source of CO, making CO a good proxy for fire plumes (eg: Edwards (2003); Sinha et al. (2004); Edwards et al. (2006); Mari et al. (2008)).(TODO: split citations to their most appropriate sentences) To identify possible biomass burning influence, we visually inspected AIRS vertical column CO in the vicinity of our three measurement sites for all dates with detected STT events. We diagnose smoke plumes as areas with elevated CO columns ($\sim 2 \times 10^{18}$ molecules cm^{-2} or higher), and flag any sonde-detected STT event that occurs near a smoke plume.

Figure 4 contrasts two days with and without signs of biomass burning influence near the Melbourne site (purple circle). On 17 October 2007 (top) elevated CO suggests the site may have been influenced by long-range transport from African and/or South American biomass burning. In contrast, on 3 February 2006 (bottom) CO columns across the Southern Hemisphere show no influence from biomass burning. We screened all days with detected STT events except one event during which there were no available AIRS data (January 2010), and found that biomass burning may have influenced 21% of events over Melbourne and 17% of events over Macquarie island. These events are flagged in the following sections, and are not used in our calculation of total STT flux. All of the flagged events except for one (in January at Macquarie Island) occur within the Southern Hemisphere burning season (July to December). No events at Davis were influenced by smoke transport.

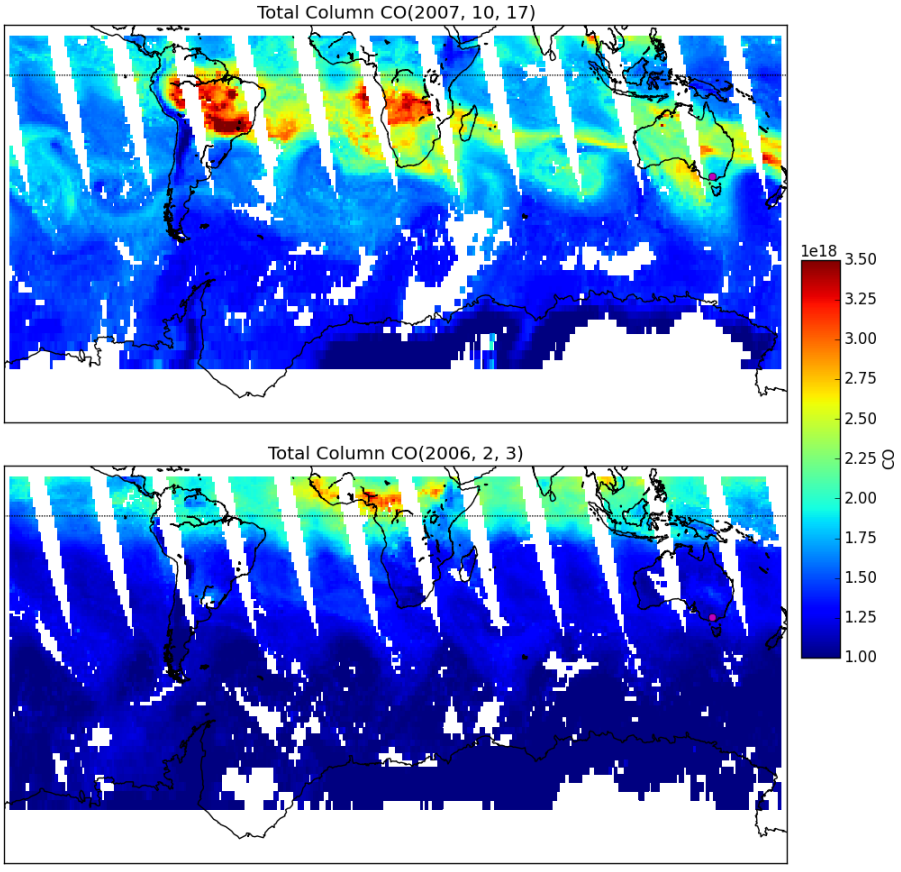

Figure 4. Example detection of biomass burning influence using AIRS total column CO. The top panel (17 October 2007) shows a day when ozone above Melbourne (purple dot) could have been caused by a transported biomass burning plume, and so was flagged in subsequent analysis. The bottom panel (3 February 2006) shows a day when Melbourne ozone was not influenced by transported smoke.

2.5 Sensitivities and limitations

Our method uses several subjectively defined quantities in the process of STT event detection. Here we briefly discuss these and the sensitivity to each. Using the algorithm discussed in Section 2.3, we detect 45 events at Davis, 47 (+8 fire influenced) events at Macquarie Island, and 72 (+14 fire influenced) events at Melbourne.

The cut-off threshold (defined separately for each site) is determined from the 99th percentile of the ozone perturbation profiles between 2 km and 1 km below the tropopause. We use the 99th percentile because at this point the filter locates clear events with no obvious false positives. Event detection is highly sensitive to this choice; for example, using the 98.5th percentile instead increased detected events by 10 (22%) at Davis, 19 (40%) at Macquarie Island, and 24 (33%) at Melbourne. This high sensitivity means that detection is also sensitive to the profile altitude bounds used in calculation of the percentiles, i.e. from

2 km altitude to 1 km below the tropopause. This range was chosen to remove anomalous edge effects of the Fourier bandpass filter and to discount the highly variable ozone concentration which occurs near the tropopause.

Ozone enhancements are only considered STT events if they occur above 4 km and within 500 m below the tropopause. This range removes possible ground pollution, as well as allowing event detection up to 500 m from the tropopause. Some likely events are removed by this range, including the storm-caused event examined below in figure 5 are within one kilometer of the tropopause.

The event detection was less sensitive to the choice of Fourier bandpass scales: a widening of the allowed scales from the range 0.5-5.0 to 0.4-5.1 increased the detected events by 3 at Melbourne and 2 at Macquarie Island, while Davis lost two events. It may seem strange that Davis lost events when the bandpass range was widened, however this was an effect of the threshold value in the perturbations filter increasing - removing some detections which weren't subsequently filtered.

Over all the method used here to detect STTs is conservative, more events can be classified however there is more chance of misdiagnosis. None of the detected events needed to be manually filtered using the described parameters.

2.6 Classifying synoptic conditions during STT events

Data from the European Center for Medium-range Weather Forecasts (ECMWF) Interim Reanalysis (ERA-I) (Dee et al., 2011) product are used for synoptic-scale examination of weather patterns over our three sites on dates matching detected STT events. We use the ERA-I 500 hPa data to subjectively classify the events based on their likely meteorological cause. Typically during STT occurrence, the upper troposphere is characterized by nearby low pressure fronts or cut-offs. Over Melbourne and Macquarie Island, we find that frontal and low pressure activity are prevalent during STT events. Over Davis, the weather systems are harder to distinguish. The stratospheric polar vortex may create ozone folds without other sources of upper tropospheric turbulence.

We examine two case studies in detail to illustrate the relationship between synoptic-scale conditions and STT events over Melbourne. Figure 5 (left) shows the ozone profile on 3 February 2005. The tropopause was between 400 and 500 hPa and ozone in the upper troposphere was anticorrelated with relative humidity, suggesting the ozone enhancements derived from dry stratospheric air. An ozone intrusion into the troposphere at $\sim$520 hPa was identified by our detection algorithm. The right panel shows the concurrent synoptic weather system, a cut-off low pressure system that caused a large storm and lowered the local tropopause height for several days. The flux of stratospheric ozone into the troposphere associated with this event, calculated using the method shown in Section 2.3, was at least 3.1×10^{11} molecules cm^{-3}, or 8% of the tropospheric ozone column.

Figure 6 (left) shows the ozone profile over Melbourne on 13 January 2010. The tropopause was higher on this date (120-160 hPa). Using our algorithm, we detected an ozone intrusion centred around 200 hPa. As before, ozone anti-correlation with relative humidity provides further evidence that the elevated ozone was stratospheric in origin. In this profile, there was clear separation between the detected intrusion (highlighted in pink) and the ozone tropopause (black dashed line), which indicates that the sonde passed through regular tropospheric air after hitting a stratospheric intrusion but before reaching the tropopause. The right panel shows that this event was associated with a trough of low pressure (front) passing over southeastern Australia.

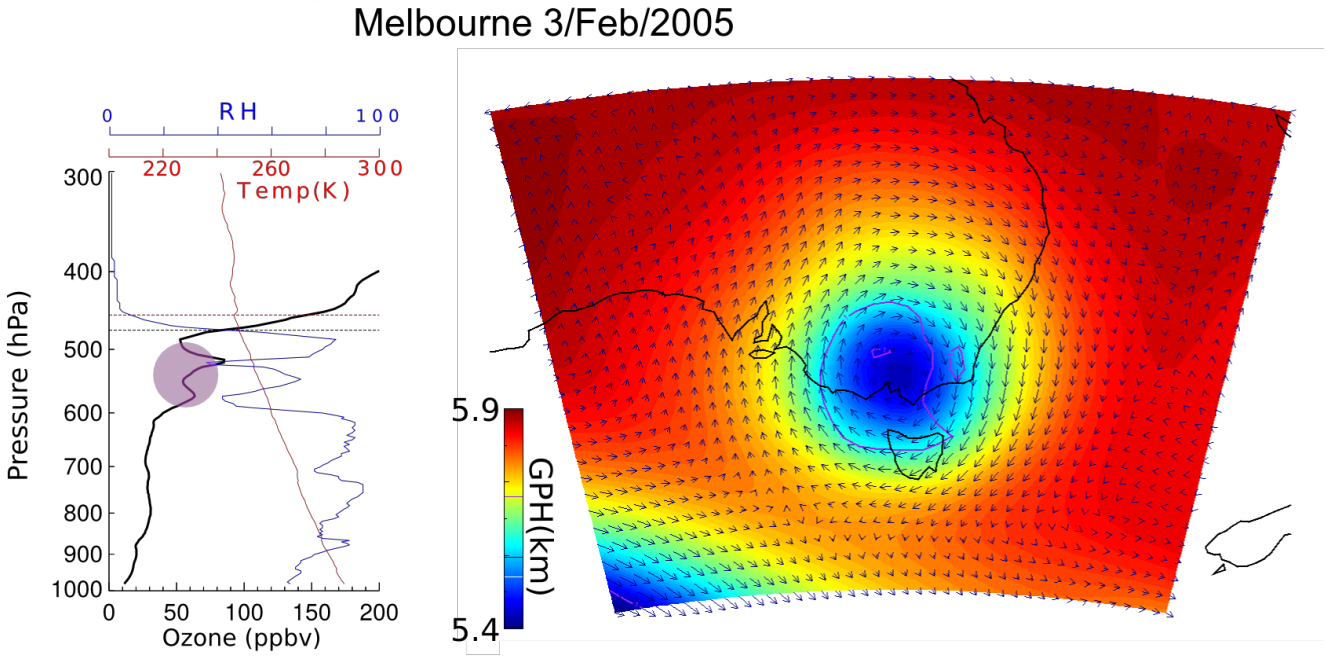

Figure 5. (Left) Vertical profile of ozone (black), relative humidity (blue), and temperature (red) measured by ozonesonde over Melbourne on 3 February 2005. The detected ozone STT event is highlighted in pink. Tropopause heights using both the ozone definition (black dashed line) and lapse rate definition (red dashed line) are also shown. (Right) Geopotential heights at 500 hPa from the ERA-Interim reanalysis, with wind vectors overplotted. Also shown are contours of potential vorticity units with 1 PVU in purple.

This front traveled from west to east and caused a wave of lowered tropopause height. Frontal passage is a known cause of STT as stratospheric air descends and streamers of ozone-rich air break off and mix into the troposphere (Sprenger et al., 2003).

3 STT event climatologies

Figure 7 shows the seasonal cycles of STT frequency at Davis, Macquarie Island, and Melbourne. Frequency is determined as detected event count divided by total launched ozonesondes for each month. STT events in Figures 7-10 are coloured based on the meteorological classification described in Section 2.6, with events classified as either low pressure fronts (“frontal”, dark blue), cut-off low pressure systems (“cutoff”, teal), or indeterminate (“misc”, cyan). Events that may have been influenced by transported smoke plumes (Section 2.4) are shown in red. Ozonesonde releases and detected event counts are summarised in table 2.

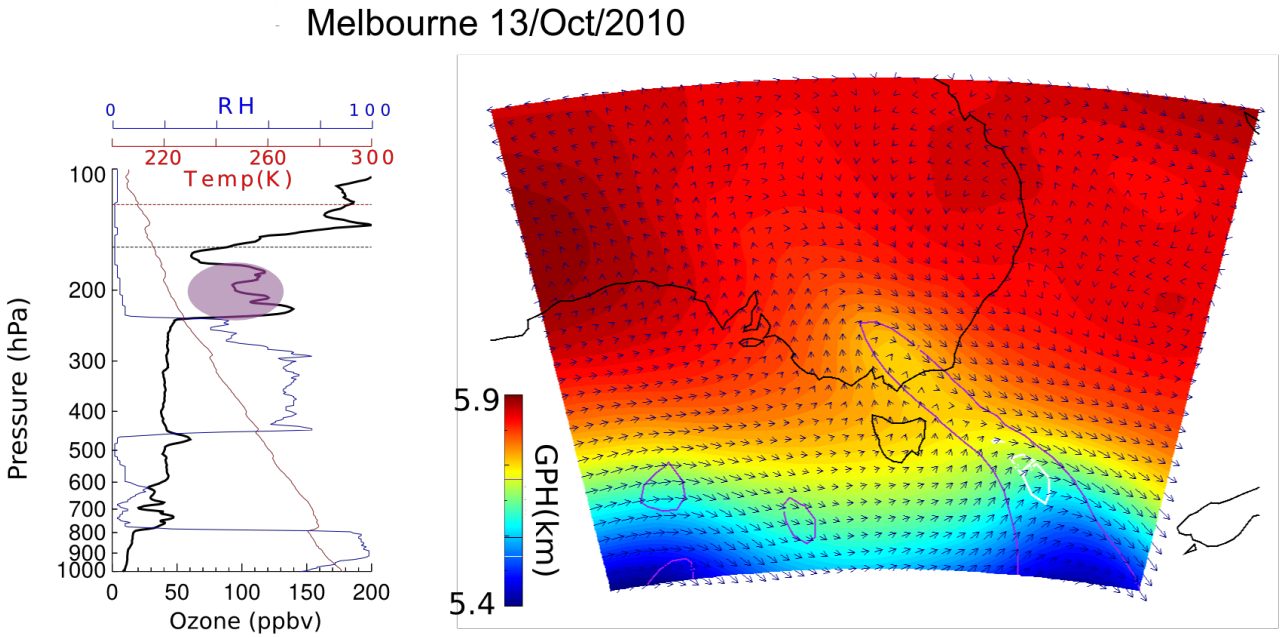

Figure 6. Same as Figure 5 but for 13 January 2010. Also shown in this figure is the 2 PVU contour (white), often used to determine dynamical tropopause height.

Site	Sondes	Events	Cut-offs	Frontals	Misc	Fire
Davis	240	45	7	20	18	0
Macquarie	390	47	10	20	9	8
Melbourne	456	72	12	34	12	14

Table 2. Total number of ozonesonde releases and detected STT events, along with the number of events in each category (see text).

There is an annual cycle in the frequency of STT events (Fig. 7) with a summertime peak above all three sites. This summertime peak is due to an increased prevalence of summer low-pressure storms and fronts, which increase turbulence and lower the tropopause (Reutter et al., 2015). For both Melbourne and Macquarie Island, the STT events (excluding fire-related) mainly occur in summer in association with these low pressure synoptic systems. At Davis, the frequency of STT events is relatively constant throughout the year, with a slight increase during Antarctic summer. STT events associated with cut-off low pressure systems are more prevalent during summer (winter for Davis), while STT events associated with frontal passage occur throughout the year. The polar vortex and associated lowered tropopause may be partially responsible for the STTs detected in winter.

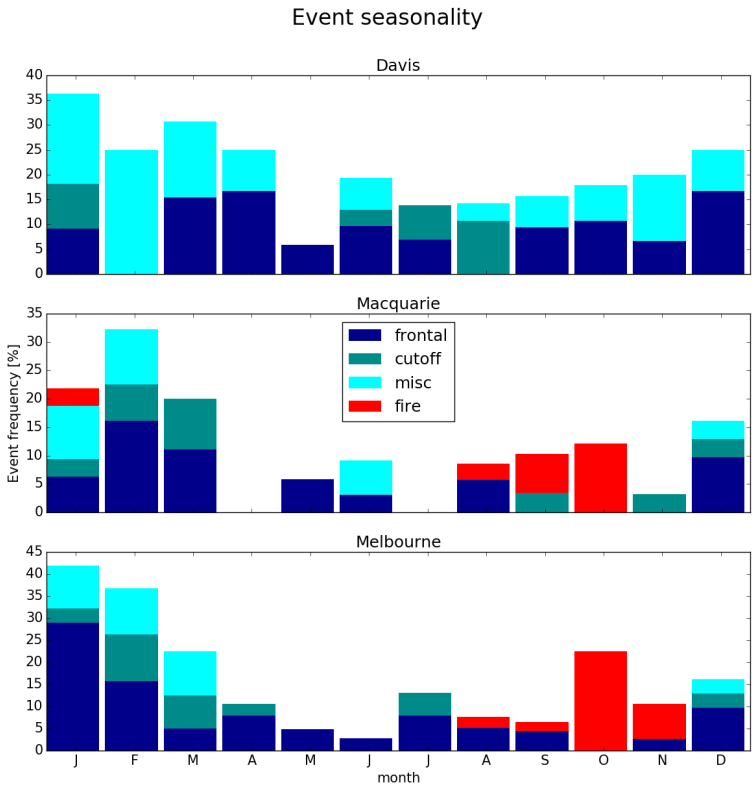

Figure 7. Seasonal cycle of STT event frequency at Davis (top), Macquarie Island (middle), and Melbourne (bottom). Events are categorised by associated meteorological conditions as described in the text, with low pressure fronts ("frontal") in dark blue, cut-off low pressure systems ("cutoff") in teal, and indeterminate meteorology ("misc") in cyan. Events that may have been influenced by transported smoke plumes are shown in red (see text for details).

To examine the robustness of the distributions shown in Fig 7, we developed an alternative assessment of the seasonal occurrence of STT events, with results shown in Figure 8. Here STT occurrence is evaluated by consideration of the square of the dry Brunt-Viäsälä frequency (N^2) at the heights of the ozone tropopause (z_{OT}) and lapse rate tropopause (z_{LRT}) in each ozonesonde profile that has been binned to 500 m resolution. We use N^2 to assess atmospheric stability, which is normally distinctly higher in the stratosphere than in the troposphere, and assume that the vertical temperature gradients within the intrusion respond most rapidly to transported heat, which is an additional characteristic of stratospheric air. The altitude binning chosen is a compromise between vertical resolution and the level of variability in N^2 introduced by temperature gradients associated with perturbations from gravity waves and changes near the lapse rate tropopause, and is the minimum that produces a robust seasonal distribution. We define STT as having taken place if $N^2(z_{OT}) > N^2(z_{LRT})$ and $z_{OT} < z_{LRT}$; in this way the characteristically higher static stability and ozone concentration of stratospheric intrusion is regarded as being retained as

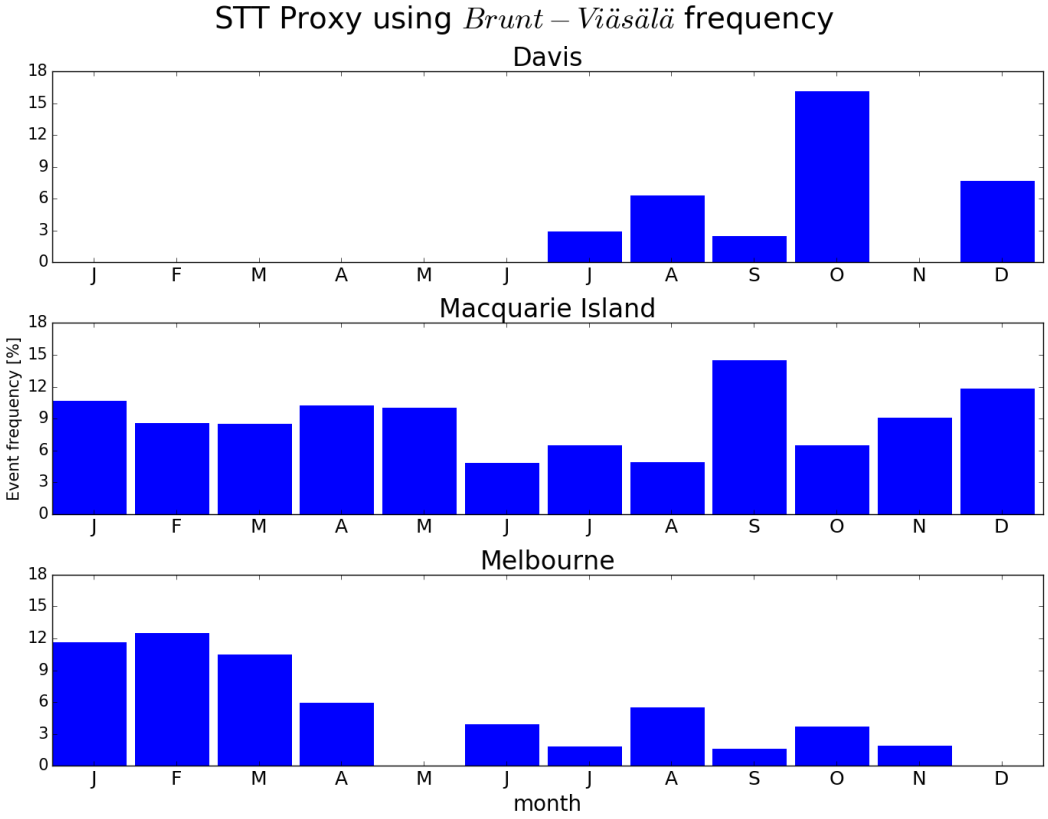

Figure 8. Seasonal distribution of the alternative STT proxy, obtained from consideration of the static stability at the ozone and lapse rate tropopauses, for Davis (2003-2012), Macquarie Island (1994-2012) and Melbourne (1999-2012).

it penetrates below the lapse rate tropopause. The seasonal distributions shown for the three stations in Fig. 8 are generally similar to those shown in Fig. 7 (although detected events are less frequent), with the main exception that no events are identified with the alternative method at Davis in the first half of the year. From December to June, ozonesondes are generally only launched monthly at Davis, and the lack of STT events in these months for Davis shown in Fig. 8 potentially reflects the fewer measurement opportunities.

Figure 9 shows the altitudes of detected events, based on the altitude of peak (maximum) tropospheric ozone in the ozonesonde profile. STT event peaks most commonly occur at 6–10 km above Melbourne and 6–9 km at Davis but are distributed more evenly at Macquarie Island from 4–7.5 km. There is no clear relationship between meteorological conditions and event altitude.

Figure 10 shows the distance from the tropopause of the event peak (using the lowest of the two tropopause definitions). The majority of STT events occur within 3 km of the tropopause at both Melbourne and Macquarie Island, and within 2 km of the tropopause at Davis. Again, there is no clear relationships between meteorological conditions and event depth.

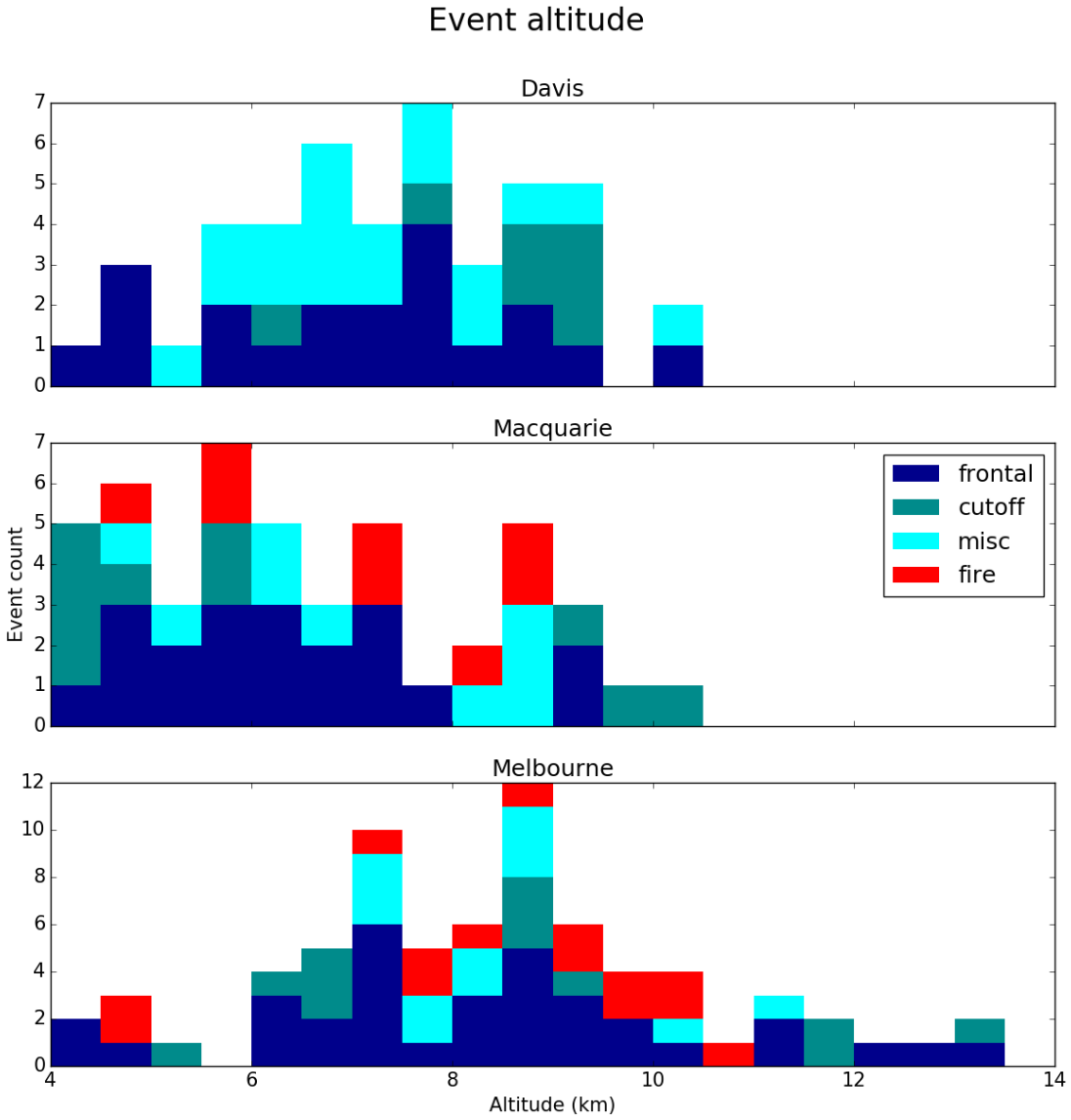

Figure 9. The distribution of STT event altitude at Davis (top), Macquarie Island (middle), and Melbourne (bottom), determined as described in the text. Events are coloured as described in Fig. 7.

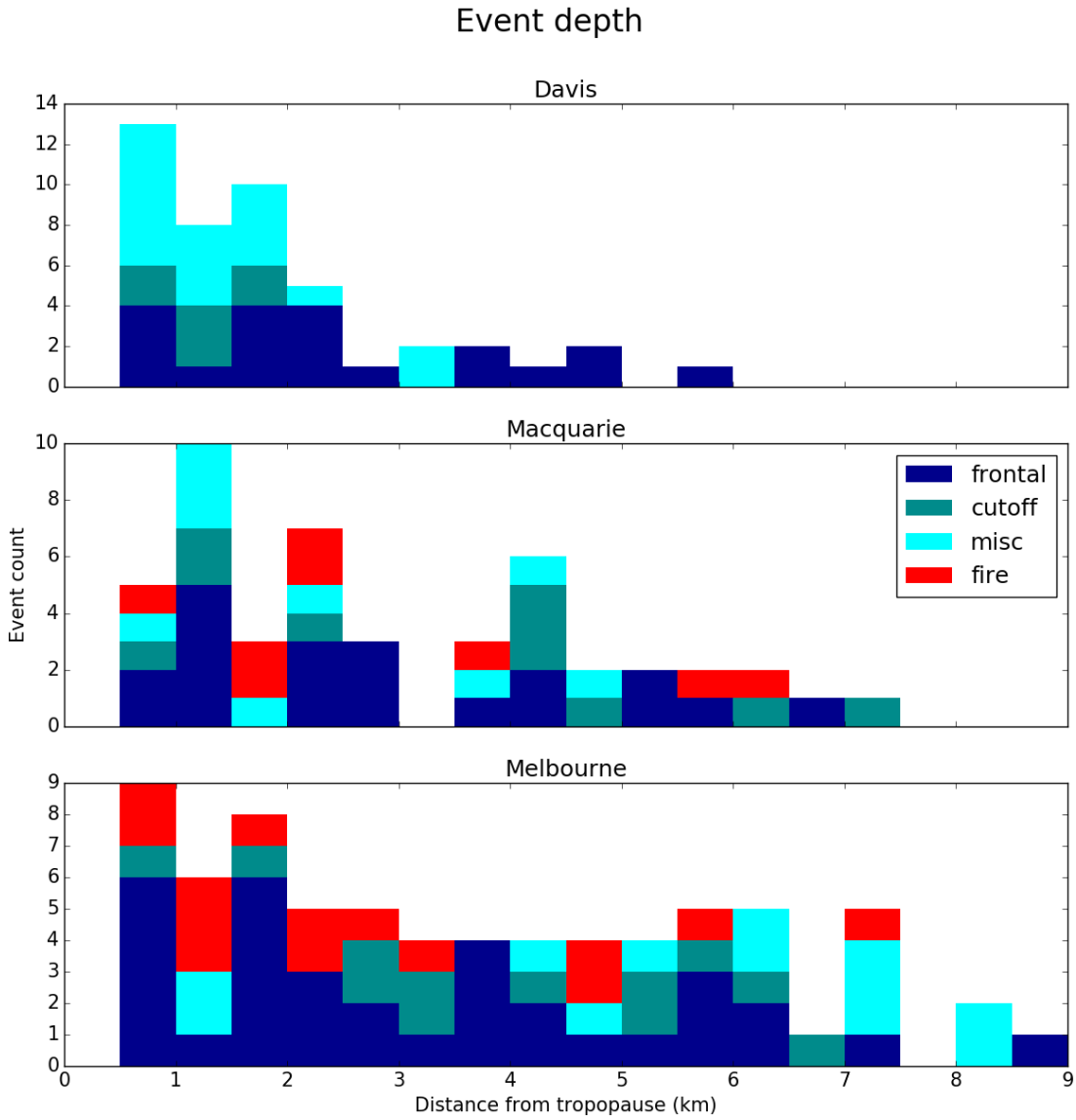

Figure 10. The distribution of STT event distance from the tropopause at Davis (top), Macquarie Island (middle), and Melbourne (bottom), determined as described in the text. Events are coloured as described in Fig. 7.

4 Simulation of southern mid-latitude ozone columns

Figure 11 compares the time series of tropospheric ozone columns (Ω_{O_3}) in molecules cm^{-2} simulated by GEOS-Chem (red) to the measured tropospheric ozone columns (black). Observed tropospheric columns are calculated from the ozonesondes

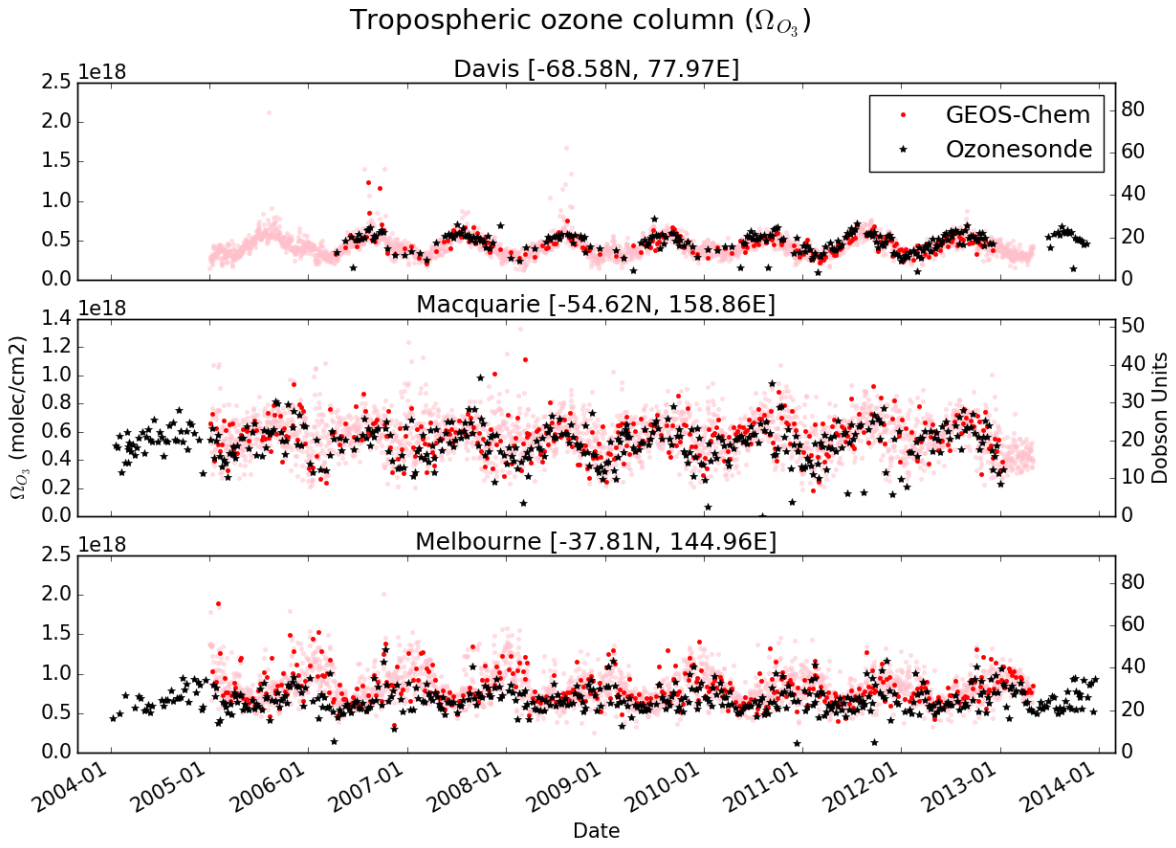

Figure 11. Comparison between observed (black) and simulated (pink, red) tropospheric ozone columns (Ω_{O3}, in molecules cm^{-2}) from 1 January 2004 to 30 April 2013. For the model, daily output is shown in pink, while output from days with ozonesonde measurements are shown in red. For each site, the model has been sampled in the relevant grid square.

by calculating the ozone number density (molec cm^{-3}) using measured ozone partial pressure (P_{O_3}) and integrating over the measured GPH up to the tropopause:

$$\mathbf{\Omega_{O_3}} = \int_0^{\mathrm{TP}} \frac{P_{O_3}(z)}{R \times T(z)} \times N_{Av} \mathrm{d}z$$

In both observations and model, the maximum ozone column at Melbourne occurs in austral summer, with a minimum in winter, while Macquarie and Davis show the opposite seasonality.

GEOS-Chem provides a reasonable simulation of the observed seasonality and magnitude of Ω_{O_3}. Reduced major axis regression of observed versus simulated Ω_{O_3} gives a line of best fit with a slopes being 1.08 for Davis, 0.99 for Macquarie,

and 1.34 for Melbourne. The model is only partially able to reproduce the variability in the observations, with paired r^2 values for of 0.38 for Davis, 0.18 for Macquarie, and 0.37 for Melbourne. Much of the variability is driven by the seasonal cycle, and after removing this effect (by subtracting the multi-year monthly means), the r^2 values decrease to .07, .11, .30 respectively, although the slope improves at Melbourne to 1.08.

Figure 12 shows the observed and simulated ozone profiles at all sites, averaged seasonally. The model generally underestimates ozone in the lower troposphere (up to 6 km) at both Davis and Macquarie, although this bias is less pronounced during summer. Over Melbourne, ozone in the lower troposphere is well represented, but the model overestimates ozone from around 4 km to the tropopause. Also shown is the tropopause height simulated by the model (horizontal dashed red line), the mean of which is always higher than the observed average, although this difference is statistically insignificant. The effect of local pollution over Melbourne during austral summer (DJF) can be seen from the increased mean mixing ratios and enhanced variance near the surface.

Although GEOS-Chem reasonably matches the ozonesonde tropospheric ozone columns, it does not have the resolution required to capture STT events. Figure 13 compares modeled (red) and observed (black) ozone profiles on three example days when STT events were detected using the ozonesondes. The figures show the profile for each site with the closest (qualitative) match between model and observations. The vertical resolution of GEOS-Chem in the upper troposphere is too low to consistently allow detection of STTs, although in a few cases (e.g. Melbourne in Figure 13) it appears that the event was large enough to be visible in the model output.

5 Stratosphere-to-troposphere ozone flux from STT events

We quantify the mean stratosphere-to-troposphere ozone flux due to STT events at each site based on the integrated ozone amount associated with each STT event (see Section 2.3). Events that may have been influenced by transported biomass burning are excluded from this calculation. Our estimate provides a very conservative lower bound as our algorithm ignores secondary ozone peaks which may also be transported from the stratosphere as well as potential ozone enhancements due to the ozone intrusion which is outside the event positive perturbation range around the detected ozone peak.

Figure 15 shows the mean fraction of total tropospheric column ozone (calculated from ozonesonde profiles) attributed to stratospheric ozone intrusions at each site, averaged over days when an STT event occurred. At all sites, the mean fraction of tropospheric ozone attributed to STT events is 2–4%. On individual days at Macquarie and Melbourne, this value can exceed 10% . Figure 14 shows the STT-induced ozone flux in absolute terms. We find that the mean ozone flux associated with STT events is 1-2 $\times 10^{16}$ molecules cm^{-2}. Our flux estimates are relatively insensitive to our biomass burning filter: including smoke-influenced days changed the mean flux by less than 5% relative to the absolute values.

We use simulated tropospheric ozone columns from GEOS-Chem to extrapolate the ozonesonde-based estimates to the entire Southern Ocean region. To do so, we multiply the monthly likelihoods of STTs (fraction of ozonesonde releases for which an STT event was detected, per month, 'l') by the monthly mean tropospheric ozone column over the Southern Ocean (from the GEOS-Chem multi-year mean, $\Omega_{SO_{O_3}}$) and by the monthly mean fraction of the ozone column attributed to STT ('f') (as in

Fig. 15, but separated by month). The monthly values of each term in this equation are shown in Figure 16 (lower panel). The equation can be written simply as Flux$= \Omega_{SO_{O_3}} \times f \times l$.

Flux estimation over the southern ocean is based on the average GEOS-Chem tropospheric vertical column of ozone over a particular latitude range. The range is from 35°S to 75°S, chosen as it captures the three measurement stations. Changing this latitude range by 5° in either direction at either end of the range changes the average simulated tropospheric ozone by -7 to 9%. A more spatially resolved estimate could be calculated, by splitting the southern ocean into longitudinal and latitudinal bins. This could include using the gradient of flux and frequency estimations along their latitudes, as well as estimated longitudinal variations such as the enhanced STE east of Australia shown in (TODO:find paper mentioned by I. Galbally). An improved spatial distribution for the flux estimation is beyond the scope of this work and would not address the limitations of the technique shown here.

Figure 16 (top) shows the extrapolated monthly mean ozone flux from STT events over the Southern Ocean. We find from this estimate that STT events may be responsible for at least 3.1×10^{16} molecules cm^{-2} yr^{-1} of the tropospheric ozone over the Southern Ocean, equivalent to 2.48 Tg yr^{-1}.

Our estimate is far less than other estimates of STT flux, due to our conservative estimate of flux within each event, as well as filtering out events which are too close to the tropopause. Previous studies have derived global gross STT fluxes of 550 Tg yr^{-1} (Stevenson et al., 2006) and net downward STT fluxes of 75 Tg yr^{-1} (Sprenger et al., 2003). Our estimate of 2.48 Tg yr^{-1} would suggest only $\sim$3.3% of the global net downward flux can be attributed to STT events, a value that is likely much too low. This result highlights one of the difficulties associated with temporally sparse ozonesonde data. Our flux calculation only detects STT events that satisfy very specific criteria, and may therefore be unsuitable for calculating large-scale STT fluxes.

Other studies have found peak STT ozone fluxes in the SH extratropics occur from autumn or winter to early spring (Olsen, 2003; Liu et al., 2016). At this time of year, we find the highest tropospheric Ω_{O3}, but a relatively low STT flux. Our results suggest instead that the ozone flux associated with STT events (at least those due to tropopause folds) is largest in austral summer (December-March), primarily due to an increased frequency of STT detections during these months. Some legitimate STT events may have been removed due to coincident smoke plumes, which could affect our STT event frequency during winter.

As described previously, our estimate of the fraction of tropospheric ozone from each STT event (f) is almost certainly biased low, perhaps by a significant amount. Using a global CTM with a stratospheric ozone tracer, Terao et al. (2008) estimated that this number was closer to 30–40%, at least for the ozone mixing ratio at 500 hPa in the northern hemisphere. If we we assume a fractional ozone flux due to each event STT event of f=35% based on their results (rather than our estimated 2-4%), our estimate of the net downward ozone STT flux from southern ocean STT events increases by an order of magnitude to $\sim$29.5 Tg yr^{-1} – 39% of the global downward flux estimated by Sprenger et al. (2003).

6 Conclusions

Stratosphere-to-troposphere transport (STT) can be a major source of ozone to the remote free troposphere, but the influence of these STT events remains poorly quantified in the southern hemisphere (SH) extratropics. Ozonesonde observations in the Southern Hemisphere provide a potential satellite-independent quantification of the ozone fluxes associated with STT events. Using almost ten years of ozonesonde profiles over the southern high latitudes, we have quantified the frequency, seasonality, and altitude distributions of STT events in the SH mid-latitudes. By combining this information with ozone column estimates with a global chemistry transport model, we provide a first, conservative estimate of the influence of STT events on tropospheric ozone over the Southern Ocean.

Our method involves applying a Fourier bandpass filter to the measured ozone profiles to identify STT events. The filter removes seasonal influences and allows clear detection of ozone-enhanced tongues of air in the troposphere. By setting empirical checks, ozonesonde vertical profiles clearly show tropospheric ozone enhancements that are separated from the stratosphere. This method is sensitive to some parameters involved in the calculation, and likely provides a lower limit on the frequency of STT events.

Our new climatology of STT events at three sites spanning the SH extra-tropics (38°S, 55°S, and 69°S shows a distinct seasonal cycle. All three sites show a summer (DJF) maximum and winter (JJA) minimum, although the seasonal amplitude is less apparent at the Antarctic site (Davis), as events are also detected regularly in winter and spring. Comparison with ERA-Interim reanalysis data suggests the majority of events are caused by turbulent weather in the upper troposphere due to low pressure fronts, followed by cut-off low pressure systems.

Vertical integration of the observed ozone enhancement also allows a rough estimate of the flux associated with each event, although this is a very conservative lower limit. We find that on average STT events are responsible for 3% of the total tropospheric ozone column, although this varies seasonally. Across all months, we conservatively estimate that the ozone enhancement due to STT events at our three sites ranges from 1 to 6×10^{16} molecules cm^{-2}.

We find that the major features of the observed time series of tropospheric ozone columns can be represented by the GEOS-Chem global chemical transport model, although the vertical resolution is not sufficient for the model to simulate STT events. Instead, we combine simulated total column ozone from the model with STT flux amounts and frequencies derived from the measurements to provide a first estimate of the total contribution of STT events to tropospheric ozone over the southern ocean. This method implies that STT events can only explain $\sim$3% of the global net downward flux of ozone, a value that is likely much too low. Replacing the sonde-derived estimate of the ozone fraction associated with each event with a value derived from a global model (Terao et al., 2008) increases this estimate by an order of magnitude.

Estimating STT flux using ozonesonde data alone remains challenging; however, the very high vertical resolution provided by ozonesondes means they are capable of detecting STT events that models, reanalyses, and satellites may not. Further work is needed to more accurately translate these ozonesonde measurements into STT ozone fluxes, particularly in the SH where data are sparse and STT is likely to be a major contributor to upper tropsopheric ozone in some regions. More frequent ozonesonde releases at SH sitewould facilitate development of better STT flux estimates for this region.

Acknowledgements. Thanks to Dr. S. Alexander who really helped get this project up and running, and thanks to Dr. M. Tully gladly shared the ozonesonde data.

References

Alexander, S. P., Murphy, D. J., and Klekociuk, A. R.: High resolution VHF radar measurements of tropopause structure and variability at Davis, Antarctica (69?? S, 78?? E), Atmospheric Chemistry and Physics, 13, 3121–3132, doi:10.5194/acp-13-3121-2013, http://www.atmos-chem-phys.net/13/3121/2013/, 2013.

Baray, J. L., Daniel, V., Ancellet, G., and Legras, B.: Planetary-scale tropopause folds in the southern subtropics, Geophysical Research Letters, 27, 353–356, doi:10.1029/1999GL010788, 2000.

Beekmann, M., Ancellet, G., Blonsky, S., De Muer, D., Ebel, A., Elbern, H., Hendricks, J., Kowol, J., Mancier, C., Sladkovic, R., Smit, H. G. J., Speth, P., Trickl, T., and Van Haver, P.: Regional and global tropopause fold occurrence and related ozone flux across the tropopause, Journal of Atmospheric Chemistry, 28, 29–44, doi:10.1023/A:1005897314623, 1997.

Bethan, S., Vaughan, G., and Reid, S. J.: A comparison of ozone and thermal tropopause heights and the impact of tropopause definition on quantifying the ozone content of the troposphere, Quarterly Journal of the Royal Meteorological Society, 122, 929–944, doi:10.1002/qj.49712253207, http://doi.wiley.com/10.1002/qj.49712253207, 1996.

Bey, I., Jacob, D. J., Yantosca, R. M., Logan, J. A., Field, B. D., Fiore, A. M., Li, Q.-B., Liu, H.-Y., Mickley, L. J., and Schultz, M. G.: Global Modeling of Tropospheric Chemistry with Assimilated Meteorology: Model Description and Evaluation, Journal of Geophysical Research, 106, 73–95, doi:10.1029/2001JD000807, 2001.

Danielsen, E. F.: Stratospheric-Tropospheric Exchange Based on Radioactivity, Ozone and Potential Vorticity, doi:10.1175/1520-0469(1968)025<0502:STEBOR>2.0.CO;2, 1968.

Das, S. S., Ratnam, M. V., Uma, K. N., Subrahmanyam, K. V., and Girach, I. A.: Influence of tropical cyclones on tropospheric ozone : possible implication, Atmospheric Chemistry and Physics (Discussions), 15, 19 305–19 323, doi:10.5194/acpd-15-19305-2015, 2016.

Dee, D. P., Uppala, S. M., Simmons, A. J., Berrisford, P., Poli, P., Kobayashi, S., Andrae, U., Balmaseda, M. A., Balsamo, G., Bauer, P., Bechtold, P., Beljaars, A. C. M., van de Berg, L., Bidlot, J., Bormann, N., Delsol, C., Dragani, R., Fuentes, M., Geer, A. J., Haimberger, L., Healy, S. B., Hersbach, H., HÃ³lm, E. V., Isaksen, L., KÃ¥llberg, P., KÃ¶hler, M., Matricardi, M., McNally, A. P., Monge-Sanz, B. M., Morcrette, J.-J., Park, B.-K., Peubey, C., de Rosnay, P., Tavolato, C., ThÃ©paut, J.-N., and Vitart, F.: The ERA-Interim reanalysis: configuration and performance of the data assimilation system, Quarterly Journal of the Royal Meteorological Society, 137, 553–597, doi:10.1002/qj.828, http://dx.doi.org/10.1002/qj.828, 2011.

Eastham, S. D., Weisenstein, D. K., and Barrett, S. R. H.: Development and evaluation of the unified tropospheric-stratospheric chemistry extension (UCX) for the global chemistry-transport model GEOS-Chem, Atmospheric Environment, 89, 52–63, doi:10.1016/j.atmosenv.2014.02.001, http://dx.doi.org/10.1016/j.atmosenv.2014.02.001, 2014.

Edwards, D. P.: Tropospheric ozone over the tropical Atlantic: A satellite perspective, Journal of Geophysical Research, 108, 4237, doi:10.1029/2002JD002927, http://doi.wiley.com/10.1029/2002JD002927, 2003.

Edwards, D. P., Emmons, L. K., Gille, J. C., Chu, A., Attié, J. L., Giglio, L., Wood, S. W., Haywood, J., Deeter, M. N., Massie, S. T., Ziskin, D. C., and Drummond, J. R.: Satellite-observed pollution from Southern Hemisphere biomass burning, Journal of Geophysical Research Atmospheres, 111, 1–17, doi:10.1029/2005JD006655, 2006.

Forster, P., Ramaswamy, V., Artaxo, P., Berntsen, T., Betts, R., Fahey, D., Haywood, J., Lean, J., Lowe, D., Myhre, G., Nganga, J., Prinn, R., Raga, G., Schulz, M., and Dorland, R. V.: Changes in Atmospheric Constituents and in Radiative Forcing. In: Climate Change 2007: The Physical Science Basis. Contribution of Working Group I to the Fourth Assessment Report of the Intergovernmental Panel on Climate Change[Solomon, S., D. Qin, M. Man, https://www.ipcc.ch/publications_and_data/ar4/wg1/en/ch2.html, 2007.

Frey, W., Schofield, R., Hoor, P., Kunkel, D., Ravegnani, F., Ulanovsky, a., Viciani, S., D'Amato, F., and Lane, T. P.: The impact of overshooting deep convection on local transport and mixing in the tropical upper troposphere/lower stratosphere (UTLS), Atmospheric Chemistry and Physics, 15, 6467–6486, doi:10.5194/acp-15-6467-2015, http://www.atmos-chem-phys.net/15/6467/2015/, 2015.

Galani, E.: Observations of stratosphere-to-troposphere transport events over the eastern Mediterranean using a ground-based lidar system, Journal of Geophysical Research, 108, 1–10, doi:10.1029/2002JD002596, http://www.agu.org/pubs/crossref/2003/2002JD002596.shtml, 2003.

Gloudemans, A., De Laat, J., Krol, M., Meirink, J. F., Van Der Werf, G., Schrijver, H., and Aben, I.: Evidence for long-range transport of carbon monoxide in the Southern Hemisphere from SCIAMACHY observations, European Space Agency, (Special Publication) ESA SP, 33, 1–5, doi:10.1029/2006GL026804, 2007.

Guenther, A. B., Jiang, X., Heald, C. L., Sakulyanontvittaya, T., Duhl, T., Emmons, L. K., and Wang, X.: The model of emissions of gases and aerosols from nature version 2.1 (MEGAN2.1): An extended and updated framework for modeling biogenic emissions, Geoscientific Model Development, 5, 1471–1492, doi:10.5194/gmd-5-1471-2012, 2012.

Jacobson, M. C. and Hansson, H.: Organic atmospheric aerosols: Review and state of the science, Reviews of Geophysics, pp. 267–294, doi:10.1029/1998RG000045, 2000.

Jaffe, D. a. and Wigder, N. L.: Ozone production from wildfires: A critical review, Atmospheric Environment, 51, 1–10, doi:10.1016/j.atmosenv.2011.11.063, http://dx.doi.org/10.1016/j.atmosenv.2011.11.063, 2012.

Langford, A. O., Brioude, J., Cooper, O. R., Senff, C. J., Alvarez, R. J., Hardesty, R. M., Johnson, B. J., and Oltmans, S. J.: Stratospheric influence on surface ozone in the Los Angeles area during late spring and early summer of 2010, Journal of Geophysical Research Atmospheres, 117, 1–17, doi:10.1029/2011JD016766, 2012.

Lefohn, A. S., Wernli, H., Shadwick, D., Limbach, S., Oltmans, S. J., and Shapiro, M.: The importance of stratospheric-tropospheric transport in affecting surface ozone concentrations in the western and northern tier of the United States, Atmospheric Environment, 45, 4845–4857, doi:10.1016/j.atmosenv.2011.06.014, http://dx.doi.org/10.1016/j.atmosenv.2011.06.014, 2011.

Lin, M., Fiore, A. M., Cooper, O. R., Horowitz, L. W., Langford, A. O., Levy, H., Johnson, B. J., Naik, V., Oltmans, S. J., and Senff, C. J.: Springtime high surface ozone events over the western United States: Quantifying the role of stratospheric intrusions, Journal of Geophysical Research Atmospheres, 117, 1–20, doi:10.1029/2012JD018151, 2012.

Liu, J., Rodriguez, J. M., Thompson, A. M., Logan, J. A., Douglass, A. R., Olsen, M. A., Steenrod, S. D., and Posny, F.: Origins of tropospheric ozone interannual variation over Réunion: A model investigation, Journal of Geophysical Research Atmospheres, pp. 1–19, doi:10.1002/2015JD023981, http://onlinelibrary.wiley.com/doi/10.1002/2015JD023981/abstract, 2015.

Liu, J., Rodriguez, J. M., Steenrod, S. D., Douglass, A. R., Logan, J. A., Olsen, M., Wargan, K., and Ziemke, J.: Causes of interannual variability of tropospheric ozone over the Southern Ocean, Atmospheric Chemistry and Physics Discussions, pp. 1–46, doi:10.5194/ACP-2016-692, 2016.

Mari, C. H., Cailley, G., Corre, L., Saunois, M., E, A., L, J., Thouret, V., and Stohl, A.: Tracing biomass burning plumes from the Southern Hemisphere during the AMMA 2006 wet season experiment, Atmos, Atmospheric Chemistry and Physics, 8, 3951–3961, doi:10.5194/acpd-7-17339-2007, 2008.

Mihalikova, M., Kirkwood, S., Arnault, J., and Mikhaylova, D.: Observation of a tropopause fold by MARA VHF wind-profiler radar and ozonesonde at Wasa, Antarctica: comparison with ECMWF analysis and a WRF model simulation, Annales Geophysicae, 30, 1411–1421, doi:10.5194/angeo-30-1411-2012, http://www.ann-geophys.net/30/1411/2012/, 2012.

Mze, N., Hauchecorne, A., Bencherif, H., Dalaudier, F., and Bertaux, J. L.: Climatology and comparison of ozone from ENVISAT/GOMOS and SHADOZ/balloon-sonde observations in the southern tropics, Atmospheric Chemistry and Physics, 10, 8025–8035, doi:10.5194/acp-10-8025-2010, 2010.

Nawahda, A.: Comments on "Global crop yield reductions due to surface ozone exposure: 1. Year 2000 crop production losses and economic damage" and " Global crop yield reductions due to surface ozone exposure: 2. Year 2030 potential crop production losses and economic, Atmospheric Environment, 71, 408–409, doi:10.1016/j.atmosenv.2012.12.045, http://dx.doi.org/10.1016/j.atmosenv.2011.01.002, 2013.

NOAA: NOAA Ozone sondes appendix, http://www.ndsc.ncep.noaa.gov/organize/protocols/appendix5/.

Olsen, M. a.: A comparison of Northern and Southern Hemisphere cross-tropopause ozone flux, Geophysical Research Letters, 30, 1412, doi:10.1029/2002GL016538, http://doi.wiley.com/10.1029/2002GL016538, 2003.

Oltmans, J., Johnson, J., Harris, M., Bendura, J., Logan, A., and Tabuadravu, J.: Ozone in the Pacific tropical troposphere from ozonesonde observations, 106, 2001.

Pak, B., Langenfelds, R., Young, S., Francey, R., Meyer, C., Kivlighon, L., Cooper, L., Dunse, B., Allison, C., Steele, L., Galbally, I., and Weeks, I.: Measurements of biomass burning influences in the troposphere over southeast Australia during the SAFARI 2000 dry season campaign, Journal of Geophysical Research D: Atmospheres, 108, SAF 16–1 – SAF 16–10, doi:10.1029/2002JD002343, http://www.scopus.com/inward/record.url?eid=2-s2.0-0742322536&partnerID=40&md5=cafaeef03b948fb456696583ed3ab9a5, 2003.

Price, J. D. and Vaughan, G.: The potential for stratosphere-troposphere exchange in cut-off-low systems, Quarterly Journal of the Royal Meteorological Society, 119, 343–365, doi:10.1002/qj.49711951007, http://onlinelibrary.wiley.com/doi/10.1002/qj.49711951007/abstract, 1993.

Reutter, P., Škerlak, B., Sprenger, M., and Wernli, H.: Stratosphere-troposphere exchange (STE) in the vicinity of North Atlantic cyclones, Atmospheric Chemistry and Physics, 15, 10 939–10 953, doi:10.5194/acp-15-10939-2015, 2015.

Selin, N. E., Wu, S., Nam, K. M., Reilly, J. M., Paltsev, S., Prinn, R. G., and Webster, M. D.: Global health and economic impacts of future ozone pollution, Environmental Research Letters, 4, 044 014, doi:10.1088/1748-9326/4/4/044014, 2009.

Sinha, P., Jaeglé, L., Hobbs, P. V., and Liang, Q.: Transport of biomass burning emissions from southern Africa, Journal of Geophysical Research, 109, D20 204, doi:10.1029/2004JD005044, 2004.

Smit, H. G. J., Straeter, W., Johnson, B. J., Oltmans, S. J., Davies, J., Tarasick, D. W., Hoegger, B., Stubi, R., Schmidlin, F. J., Northam, T., Thompson, A. M., Witte, J. C., Boyd, I., and Posny, F.: Assessment of the performance of ECC-ozonesondes under quasi-flight conditions in the environmental simulation chamber: Insights from the Juelich Ozone Sonde Intercomparison Experiment (JOSIE), Journal of Geophysical Research Atmospheres, 112, 1–18, doi:10.1029/2006JD007308, 2007.

Sprenger, M., Croci Maspoli, M., and Wernli, H.: Tropopause folds and cross-tropopause exchange: A global investigation based upon ECMWF analyses for the time period March 2000 to February 2001, Journal of Geophysical Research: Atmospheres, 108, n/a—-n/a, doi:10.1029/2002JD002587, http://dx.doi.org/10.1029/2002JD002587, 2003.

Stevenson, D. S., Dentener, F. J., Schultz, M. G., Ellingsen, K., van Noije, T. P. C., Wild, O., Zeng, G., Amann, M., Atherton, C. S., Bell, N., Bergmann, D. J., Bey, I., Butler, T., Cofala, J., Collins, W. J., Derwent, R. G., Doherty, R. M., Drevet, J., Eskes, H. J., Fiore, A. M., Gauss, M., Hauglustaine, D. A., Horowitz, L. W., Isaksen, I. S. A., Krol, M. C., Lamarque, J.-F., Lawrence, M. G., Montanaro, V., Müller, J.-F., Pitari, G., Prather, M. J., Pyle, J. A., Rast, S., Rodriguez, J. M., Sanderson, M. G., Savage, N. H., Shindell, D. T., Strahan, S. E., Sudo, K., and Szopa, S.: Multimodel ensemble simulations of present-day and near-future tropospheric ozone, J. Geophys. Res., 111, doi:10.1029/2005jd006338, http://dx.doi.org/10.1029/2005JD006338, 2006.

Stohl, A., Wernli, H., James, P., Bourqui, M., Forster, C., Liniger, M. A., Seibert, P., and Sprenger, M.: A new perspective of stratosphere-troposphere exchange, Bulletin of the American Meteorological Society, 84, 1565–1573+1473, doi:10.1175/BAMS-84-11-1565, 2003.

Tang, Q. and Prather, M. J.: Correlating tropospheric column ozone with tropopause folds: The Aura-OMI satellite data, Atmospheric Chemistry and Physics, 10, 9681–9688, doi:10.5194/acp-10-9681-2010, 2010.

Tang, Q. and Prather, M. J.: Five blind men and an elephant: can NASA Aura measurements quantify the stratosphere-troposphere exchange of ozone flux?, Atmospheric Chemistry and Physics, 11, 2357–2380, doi:10.5194/acp-12-2357-2012, http://dx.doi.org/10.5194/acpd-11-26897-2011, 2012.

Terao, Y., Logan, J. A., Douglass, A. R., and Stolarski, R. S.: Contribution of stratospheric ozone to the interannual variability of tropospheric ozone in the northern extratropics, J. Geophys. Res., 113, doi:10.1029/2008jd009854, http://dx.doi.org/10.1029/2008jd009854, 2008.

Texeira, J.: AIRS/Aqua L3 Daily Standard Physical Retrieval (AIRS-only) 1 degree x 1 degree V006: Accessed 2/Dec/2015, doi:doi:10.5067/AQUA/AIRS/DATA303, 2013.

Thompson, A. M., Balashov, N. V., Witte, J. C., Coetzee, J. G. R., Thouret, V., and Posny, F.: Tropospheric ozone increases over the southern Africa region: Bellwether for rapid growth in Southern Hemisphere pollution?, Atmospheric Chemistry and Physics, 14, 9855–9869, doi:10.5194/acp-14-9855-2014, 2014.

Tomikawa, Y., Nishimura, Y., and Yamanouchi, T.: Characteristics of Tropopause and Tropopause Inversion Layer in the Polar Region, SOLA, 5, 141–144, doi:10.2151/sola.2009-036, http://dx.doi.org/10.2151/sola.2009-036, 2009.

Vaughan, G., Price, J. D., and Howells, A.: Transport into the troposphere in a tropopause fold, Quarterly Journal of the Royal Meteorological Society, 120, 1085–1103, doi:10.1002/qj.49712051814, 1993.

Wirth, V.: Diabatic heating in an axisymmetric cut-off cyclone and related stratosphere-troposphere exchange, Quarterly Journal of the Royal Meteorological Society, 121, 127–147, doi:10.1002/qj.49712152107, http://doi.wiley.com/10.1002/qj.49712152107, 1995.

WMO, W. M. O.: Meteorology A Three-Dimensional Science, Geneva, Second Session of the Commission for Aerology, 4, 134–138, 1957.

Zhang, L., Jacob, D. J., Yue, X., Downey, N. V., Wood, D. A., and Blewitt, D.: Sources contributing to background surface ozone in the US Intermountain West, Atmos. Chem. Phys., 14, 5295–5309, doi:10.5194/acp-14-5295-2014, http://dx.doi.org/10.5194/acp-14-5295-2014, 2014.

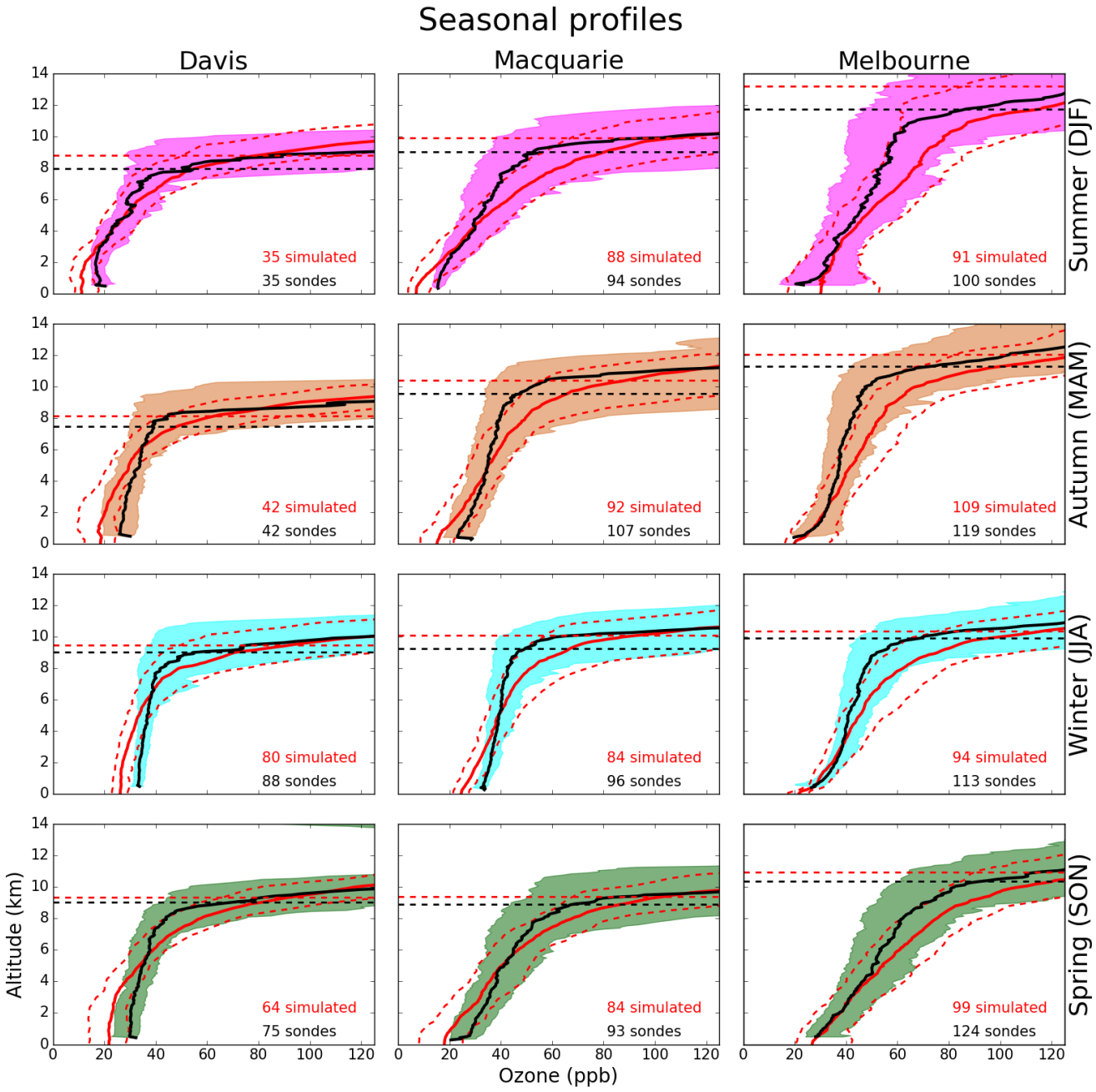

Figure 12. Observed and simulated tropospheric ozone profiles over Davis, Macquarie, and Melbourne, averaged seasonally. Model means (2005-2013 average) are shown as red solid lines, with red dashed lines showing the 10th and 90th percentiles. Ozonesonde means (over each season, for all years) are shown as black solid lines, with coloured shaded areas showing the 10th and 90th percentiles. The horizontal dashed lines show the mean tropopause heights from the model (red) and the observations (black).

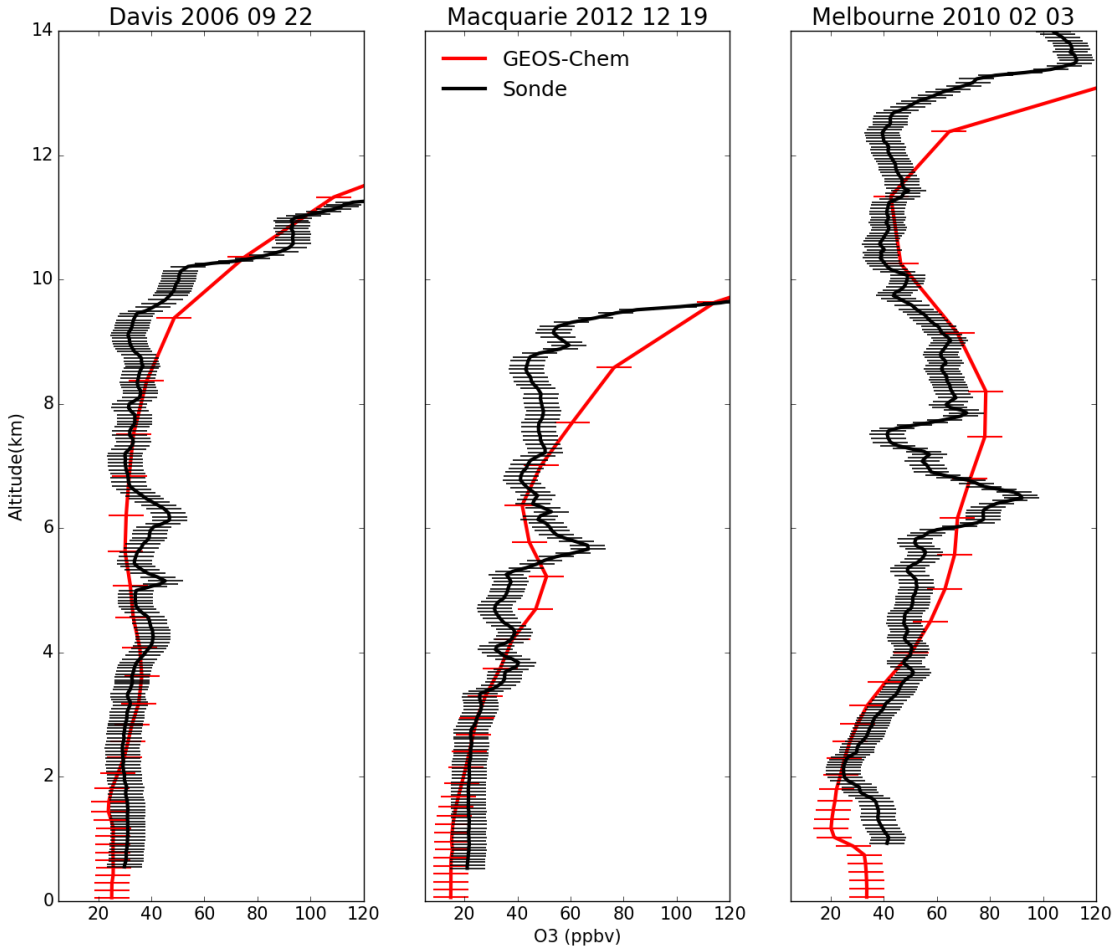

Figure 13. Example comparisons of ozone profiles from ozonesondes (black) and GEOS-Chem (red) from three different dates during which STT events were detected from the measurements. The dates were picked based on subjective visual analysis. The examples show the best match between model and observations for each site. GEOS-Chem pressure levels are marked with a dash.

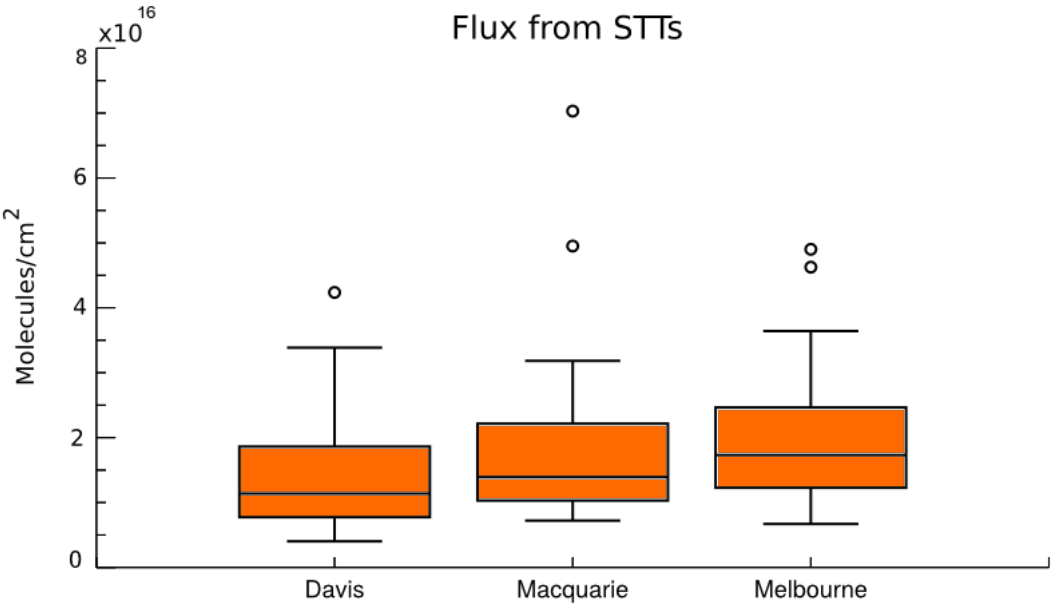

Figure 14. Tropospheric ozone attributed to STT events, derived from ozonesonde measurements as described in the text. Box shows the interquartile range (IQR), with the centre line being the median, whiskers show the minimum and maximum, circles show values which lie more than 1.5 IQR from the median.

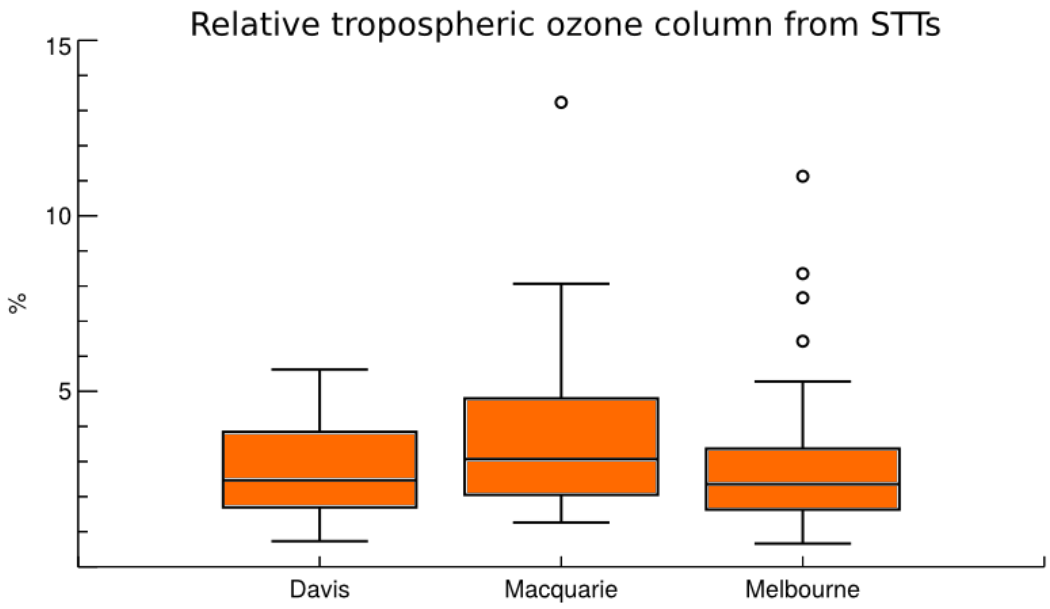

Figure 15. Percent of total tropospheric column ozone attributed to STT events, derived from ozonesonde measurements as described in the text.

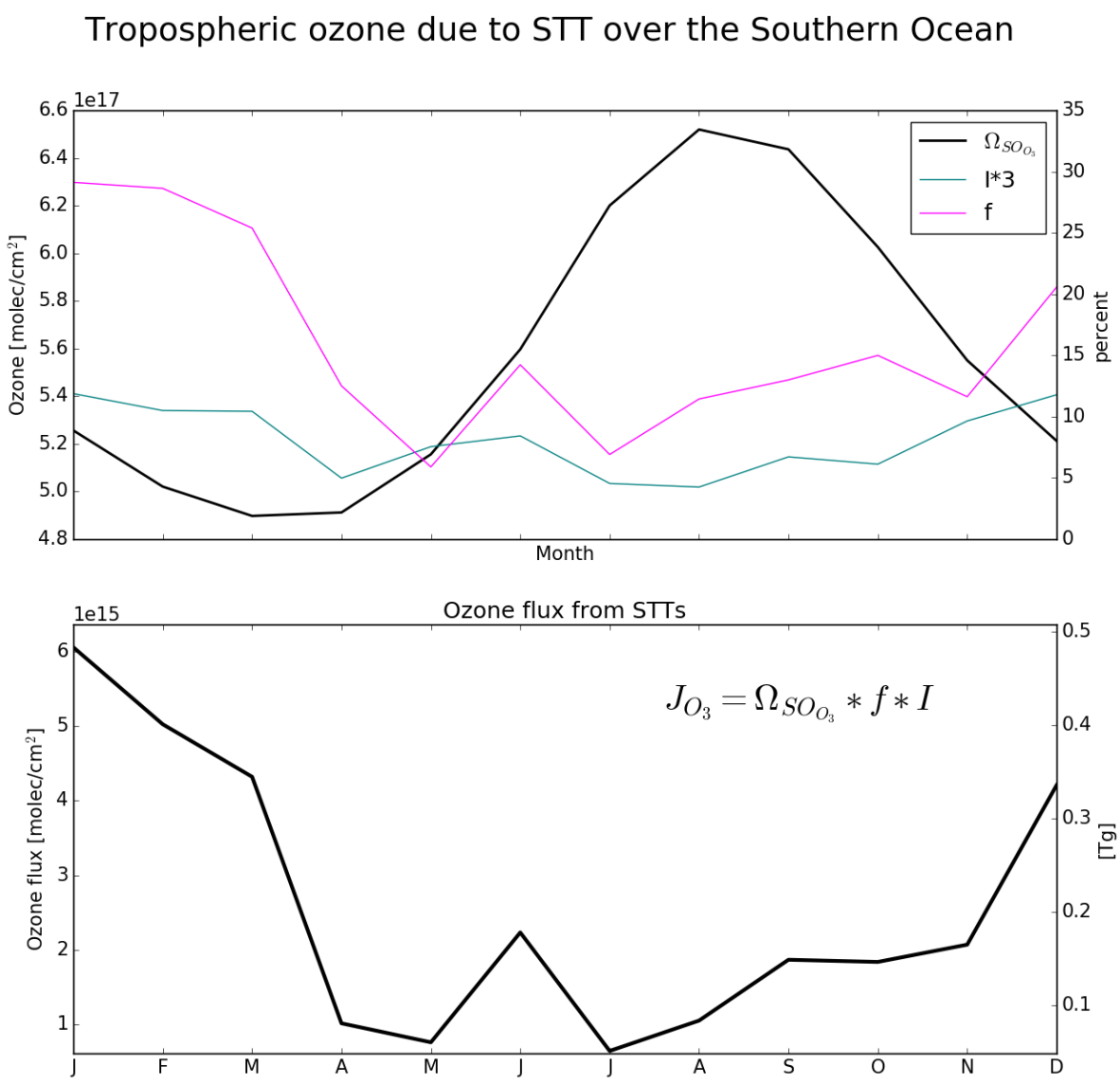

Figure 16. (Top) Estimated contribution of STT to tropospheric ozone columns over the Southern Ocean. (Bottom) The three quantities used to calculate (as per the text) the flux estimates shown in the top panel. The tropospheric ozone column $\Omega_{SO_{O_3}}$ (black, left axis) is from GEOS-Chem, while the STT fraction f (blue, right axis) and likelihood l (purple, right axis) are from the ozonesonde measurements. The STT fraction is multiplied by 3 to show the seasonality.